Stabilization of Spatiotemporal Dissipative Solitons in Multimode Fiber Lasers by External Phase Modulation

Vladimir L. Kalashnikov* and Stefan Wabnitz†
Dipartimento di Ingegneria dell'Informazione, Elettronica e Telecomunicazioni, Sapienza Università di Roma, via Eudossiana 18, 00184 Rome, Italy
(Dated: May 8, 2023)

In this work, we introduce a method for the stabilization of spatiotemporal solitons. These solitons correspond to light bullets in multimode optical fiber lasers, or localized coherent patterns in Bose-Einstein condensates. We show that a three-dimensional confinement potential, formed by a two-dimensional graded refractive index including radially-graded dissipation, in combination with external temporal phase modulation, may permit the generation of stable spatiotemporal dissipative solitons. This corresponds to combining harmonic mode-locking with the distributed Kerr-lens mode locking mechanism. Our study of the soliton characteristics and stability is based on analytical and numerical solutions of the generalized dissipative Gross-Pitaevskii equation. This approach could lead to higher energy (or condensate mass) harvesting in coherent spatio-temporal beam structures formed in multimode fiber lasers (or weakly-dissipative Bose-Einstein condensates).

I. INTRODUCTION

Research progress in mastering stable multidimensional wave patterns [1–3] has an interdisciplinary character. It bridges across different phenomena in both physical and social sciences, ranging from photonics (so-called "light bullets," LBs, or spatiotemporal optical solitons) [4–6], Bose-Einstein condensates (BECs) [7, 8], plasma confinement [9], "living matter" [10], socio-technical systems [11], and many other fields [12, 13]. In photonics and BEC, multidimensional soliton-like structures could provide unprecedented energy (or mass) condensation [14–16], as well as breakthroughs in the information capacity of photonic networks [17], and mastering of multimode microresonators for optical comb generation and optomechanics [18, 19].

The main issue hampering the practical use of multidimensional soliton-like structures is given by their intrinsic instability [20], which leads to the formation of filaments, rogue-wave-like and turbulent structures [21, 22]. This challenge becomes crucial when the number of transverse and longitudinal modes in multimode fibers (MMFs) grows larger, owing to the loss of coherence between modes, and the resulting unprecedentedly complex mode-beating dynamics [22–24]. Several methods for addressing multi-dimensional soliton instabilities have been recently proposed. Basic approaches involve the use of "trapping potentials" (e.g., in photonics, a graded refractive index, or GRIN, fiber can be used) [8, 25, 26]. In combination with Kerr nonlinearity (or attractive boson interaction in BEC), such potentials could provide transverse-mode stabilization, and even spatiotemporal soliton or light bullet (LB) formation [27, 28].

However, energy (or mass for BEC) harvesting involves the interaction with an environment (i.e., a "basin"). Such systems must be dissipative, and stable emerging soliton-like structures should belong to the class of the so-called dissipative solitons (DSs) [13]. As it was earlier pointed out, dissipative nonlinearities can stabilize both spatial and spatiotemporal (ST) DSs [29–33]: such mechanisms could be enhanced, in particular, by gain localization [33–36]. Nevertheless, until now an endeavor for demonstrating true ST 3D-DSs remains challenging, because it requires using some additional mode-locking (i.e., dissipative nonlinearity) mechanisms for its operation (e.g., see [29, 37]).

An alternative mechanism has been proposed for multidimensional soliton stabilization: it is based on nonlinear transverse mode coupling in fiber arrays [38–40] or in tapered multicore fibers [41]. Such a mechanism requires changing a basic paradigm: nonlinearity (e.g., Kerr-nonlinearity in photonics, or attractive boson interaction in BECs) must be enhanced rather than suppressed [42]. Such a change of approach (see [43]) was implemented by means of the so-called distributed Kerr-lens mode-locking (DKLM) technique. DKLM allows for the effective energy harvesting of femtosecond pulses in thin-disk solid-state oscillators, operating in both normal or anomalous chromatic dispersion regimes [44]. The obvious resource for energy harvesting is the up-scaling of the laser mode size, which is prone to introduce multimode instabilities. Therefore, the soliton stabilization mechanism based on increasing the level of nonlinearity was called "ST mode-locking" (STML), ultimately leading to LB or ST soliton generation [43].

As it was recently shown in [15], the concept of STML could be implemented as DKLM in a GRIN MMF laser, with transverse grading of both refractive index and dissipation. The complex confinement potential in [15] corresponds to a cigar-like confining potential in a weakly-dissipative BEC (Fig. 1, a) [16]. As it was previously found, an external periodical phase modulation can substantially enhance 1D-soliton stability in a dissipative system in the presence of Kerr-nonlinearity [45–49]. Such a modulation involves, in particular, a periodic change of

* vladimir.kalashnikov@uniroma1.it
† stefan.wabnitz@uniroma1.it

the refractive index over a laser cavity round-trip [50]. In a fiber laser, a synchronous external phase modulation corresponds to harmonic mode-locking. This leads to a 3D, pancake-like potential which confines LBs in both spatial and temporal dimensions (Fig. 1, b), thus facilitating total mode-locking, or simultaneous transverse and longitudinal mode-locking [14]. In this work, we theoretically study how the presence of a 3-D potential affects ST soliton stability. By optimizing other dissipative parameters, we demonstrate that external phase modulation enhances LB stability. We show that, on the one hand, periodic phase modulation may even suppress LB formation; on the other hand, it may permit to support stable LBs without the need for introducing graded dissipation.

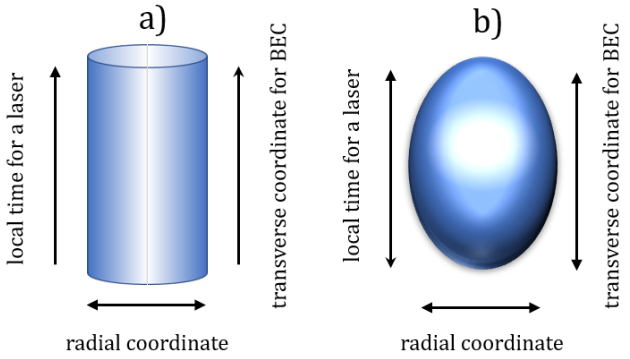

FIG. 1. Schematic illustration of complex confining potentials of either cigar- (a) or pancake-like (b) shape in GRIN MMFs or BEC. Here the transverse coordinate z in the (z, r)- frame for BECs is analogous to local time t in the (t, r)- frame for a laser operating in the anomalous dispersion regime.

II. MODEL AND ANALYTICAL SOLITON SOLUTIONS

A. Generalized dissipative Gross-Pitaevskii equation

Well-established approaches use the Gross-Pitaevskii (GPE) for modeling the evolution of either the electric field in GRIN MMFs, or matter dynamics BECs, in the presence of a confining external potential [5, 8, 23, 28]. We build here on a generalized GPE model, taking into account the presence of both dissipative effects [15, 16] and of a 3D or pancake-like confining potential (Fig. 1, b):

$$i\frac{\partial a}{\partial \xi} = -\frac{1}{2}\left[\frac{1}{r}\frac{\partial}{\partial r}r\frac{\partial}{\partial r} + (1-2i\tau)\frac{\partial^2}{\partial \chi^2}\right]a + \\ +\frac{1}{2}(1-2i\kappa)\,r^2 a + \nu\chi^2 a - |a|^2 a - i\Lambda a. \qquad (1)$$

Here, ξ stands for either time T for BECs, or the propagation coordinate Z for a MMF laser, respectively. Moreover, r is a radial coordinate under the condition of axial symmetry; the first term in square brackets describes diffraction in photonics, or the contribution of the transverse component of boson kinetic energy in BECs. χ is a local time coordinate t in a co-moving coordinate frame in photonics, or a longitudinal spatial coordinate z in BECs. Then, the $\partial^2/\partial\chi^2$-term describes anomalous group-velocity dispersion in photonics, or the contribution of the longitudinal component of boson kinetic energy in BECs. The pancake-like (i.e., r, χ-dependent) parabolic confining potential is provided by the GRIN structure, and a synchronous external temporal phase modulation parameter ν. Such confinement is supported by a transversely graded dissipation, defined by the κ-parameter, leading to effective on axis ($r = 0$) gain ($\Lambda < 0$). For BECs, a "gain" means an inflow from a non-coherent "reservoir" [16, 51]. We assume no dissipation confinement along the t/z-axis (i.e., no active ML or short-scale gain localization in a laser, or geometry of the confining lattice in BECs [51, 52]). The nonlinear self-interaction term $|a|^2 a$ is defined by the self-phase modulation strength in photonics, or the two-body scattering length ("attracting") in BECs. The spectral dissipation in a laser (or "kinetic cooling" along the dissipative unconfined $z-$axis in BECs) is defined by the $\tau-$parameter.

Eq. (1) is dimensionless, and the normalization rules for photonics correspond to those in [15, 53]: the transverse spatial coordinate is normalized to $w_0 = 1\Big/\sqrt[4]{2k_0\,|n_1|\,\beta_0}$, where $k_0 = \omega_0/c$, $\beta_0 = n(\omega_0)\,k_0$ (ω_0 is a carrier frequency, c is the light speed in vacuum, $n(\omega_0)$ is a refractive index on the axis $r = 0$, and $|n_1|$ is a measure of refractive index chance along the $r-$direction). The propagation length is normalized to $L_d = \beta_0 w_0^2$, and the co-moving frame is defined as $t = (T - \beta_1 Z)/T_0$ (β_1 is a group-velocity coefficient). Local time t is normalized to $T_0 = \sqrt{|\beta_2|\,L_d}$, where β_2 is a group-velocity dispersion coefficient. The field amplitude normalization scale is $\sqrt{k_0 n_2 L_d}$, where n_2 is a Kerr nonlinear coefficient.

B. Variational approximation

One may conjecture that the desired result of multimode synthesizing is close to a fundamental mode [27]. In this case, the powerful variational technique could be used [15, 16, 53, 54]. The corresponding ansatz for a LB without vorticity charge can be written as:

$$a(Z,r,t) = \alpha(Z)\,\exp\left[i\left(\phi(Z) + \psi(Z)\,t^2 + \theta(Z)\,r^2\right)\right]\times \\ \times\mathrm{sech}\left(\frac{t}{\upsilon(Z)}\right)\exp\left[-\frac{r^2}{2\rho(Z)^2}\right], \qquad (2)$$

where the propagation distance or $Z-$dependent parameters are defined as follows: α is the LB amplitude, ϕ is

a phase, ψ and θ are temporal and spatial chirps, respectively, υ is the LB temporal width, and ρ is the beam size.

The generating Lagrangian for the non-dissipative part of Eq. (1) is

$$L = \frac{i}{2}\left[a^*\partial_Z a - a\,\partial_Z a^*\right] + \frac{1}{2}\left(|\partial_t a|^2 + |\partial_x a|^2 + |\partial_y a|^2\right) + \frac{1}{2}\left[\left(x^2+y^2\right) + \nu\, t^2\right]|a|^2 - \frac{1}{2}|a|^4, \tag{3}$$

where the Cartesian coordinates are restored: $x = r\cos(\vartheta)$, $y = r\sin(\vartheta)$ ($r = \sqrt{x^2+y^2}$, and ϑ are the radial and azimuthal cylindrical coordinates, respectively).

The driving "force" is defined by the dissipative terms in Eq. (1):

$$Q = -i\left[\Lambda\, a + \tau\,\partial_{t,t} a - \kappa\left(x^2+y^2\right)\right] a. \tag{4}$$

The Euler-Lagrange-Kantorovich equation reads as [55]:

$$\frac{\delta\tilde{L}}{\delta \mathrm{f}} - \frac{d}{dZ}\frac{\delta\tilde{L}}{\delta \mathrm{f}} = 2\Re\int_{-\infty}^{\infty}\int_{0}^{\infty}\int_{0}^{2\pi} r\,Q\,\frac{\delta a}{\delta \mathrm{f}}\,dt\,dr\,d\vartheta, \tag{5}$$

where the variation for the reduced Lagrangian

$$\tilde{L} = \int_{-\infty}^{\infty}\int_{0}^{\infty}\int_{0}^{2\pi} r\,L\,dt\,dr\,d\vartheta, \tag{6}$$

was performed, after substituting the ansatz (2) in L and Q, over the $Z-$dependent parameters $\mathrm{f} = (\alpha,\ \phi,\ \theta,\ \psi,\ \upsilon,\ \rho)$ of (2).

C. Spatio-temporal dissipative solitons

From some algebra with (2,5) (see [56]), we obtained the following expressions for the 2D-DS parameters:

$$\theta = -\frac{\kappa\rho^2}{2},\ \psi = \frac{120\tau}{\pi^2\left(\sqrt{15}\sqrt{\upsilon^4\left(15+128\tau^2\right)} + 15\upsilon^2\right)},$$
$$\alpha^2 = \frac{3(1-\rho^4-\kappa^2\rho^8)}{\rho^2}, \tag{7}$$
$$\upsilon^2 = \frac{15\left(\sqrt{1920\tau^2+225}-15\right) - 64\left(15+2\pi^2\right)\tau^2}{384\pi^2\tau(\kappa\rho^2+\Lambda)}.$$

The value of ϕ is irrelevant in our context. However, its value could be interesting for a stability analysis, based on the Vakhitov-Kolokolov stability criterion [25].
The remaining equation for the beam size ρ:

$$\frac{3\left(64\left(15+2\pi^2\right)\tau^2 - 15A + 225\right)\left(\kappa^2\rho^8+\rho^4-1\right)}{128\pi^2\rho^2\tau(\kappa\rho^2+\Lambda)} + \frac{\left(64\left(15+2\pi^2\right)\tau^2 - 15A + 225\right)^2\nu}{49152\pi^2\tau^2(\kappa\rho^2+\Lambda)^2} - \frac{80\left(\pi^2\left(3+\pi^2\right)(A+15) - 1080\right)\tau^2}{\pi^4(A+15)^2} = 6, \tag{8}$$
$$A = \sqrt{1920\tau^2+225}.$$

can be numerically solved.

The dependencies of the DS width and energy on the dissipation gradient parameter κ, for different values of Λ, τ, and ν, are shown in Figs. 2, 3.

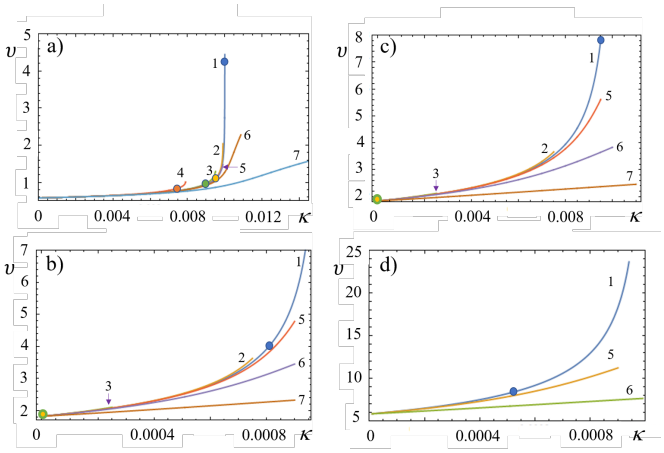

FIG. 2. Dependencies of the DS temporal width υ on the dissipation gradient parameter κ. τ =0.01 (a, b), 0.1 (c, d); Λ =-0.01 (a, c), -0.001 (b, d). The curves correspond to different values of the phase modulation parameter ν =0 (1), 0.001 (2), 0.01 (3), 0.1(4), -0.001 (5), -0.01 (6), -0.1 (7). The colored points show the minimal $\kappa-$parameter, which is required for DS stabilization (colors refer to the color of the corresponding curve, see Table 1).

Figs. 2, 3 demonstrate a clear division between the DS branches corresponding of a positive $\nu > 0$ ("guiding", curves 2 –4) or a negative $\nu < 0$ ("anti-guiding", curves 5 –7) phase modulation parameter, respectively. Such a difference is due the self-focusing type of nonlinearity, and the anomalous chromatic dispersion. Namely, $\nu > 0$ contributes additively to the DS chirp, which reduces the overall nonlinear phase shift, in agreement with the chirp-free condition (see Appendix, Eq. (A2)):

$$\frac{2}{\upsilon^2} = \pi^2\nu\upsilon^2 + \alpha^2 \tag{9}$$

As a consequence, $\nu > 0$ leads to the a decrease of the peak power and energy E of the DS. One must note that the DS width remains almost unaffected in this case, but the range of DS existence vs. the $\kappa-$parameter shrinks.

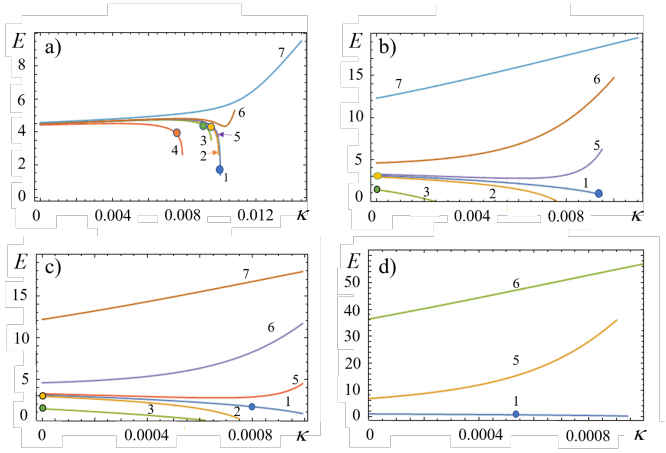

FIG. 3. Dependencies of the DS energy E on the dissipation gradient parameter κ. All remarks correspond to Fig. 2.

The opposite situation takes a place for a negative phase modulation coefficient ν <0: here the DS energy E increases, and simultaneously the DS width υ decreases.

D. Spatiotemporal soliton stability analysis

In order to analyze the stability of solutions (7,8), we numerically evaluated the generating system (A1 – A5) (see Appendix). The calculated evolution of the DS width and intensity in the vicinity of the stability boarders, marked by circles in Figs. 2, 3, are illustrated by Figs. 4–7. The stability properties obtained from these simulations are summarized in Table I. The initial conditions on Z =0 are $\alpha_0 = 0.01$, $\theta_0 = \psi_0 = 0$, $\upsilon_0 = \sqrt{2}/\alpha_0$, $\rho_0 = \left(\alpha_0 - \sqrt{\alpha_0^4 + 36}\right)/6$ [15].

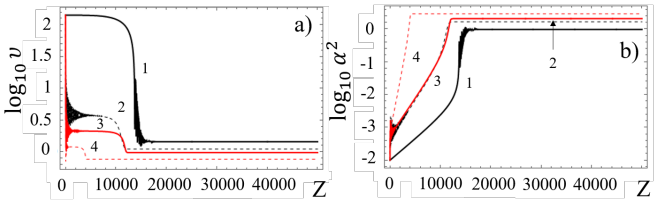

FIG. 4. Evolution of the DS temporal width (a) and intensity (b), in the vicinity of the stability threshold (i.e., the minimal κ, as pointed by circles in Figs. 2, 3), for the parameters of Figs. 2, 3, a.

From our numerical analysis, we may note the following three main results: i) there is a maximum phase modulation parameter ν, for which there is no DS solution, ii) there is no DS for ν <0, iii) the action of phase modulation ($\nu \neq$0) broadens the DS stability range with respect to the graded dissipation parameter κ, down to its zero level (i.e., a gain/loss profiling is no longer required in this case).

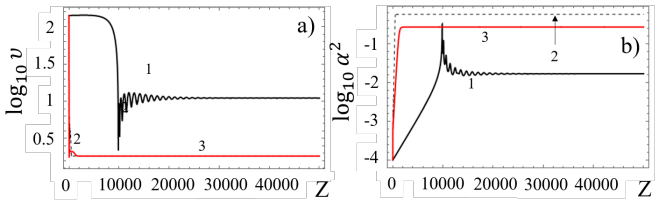

FIG. 5. Evolution of the DS temporal width (a) and intensity (b), in the vicinity of stability threshold (i.e., minimal κ, as pointed by circles in Fig. 2, 3), for the parameters of Fig. 2, 3, c.

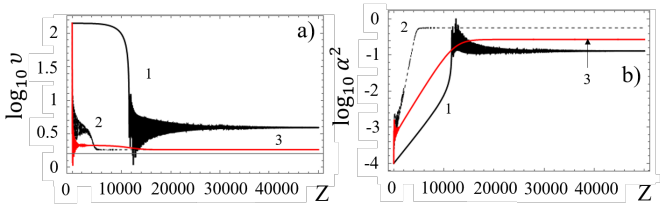

FIG. 6. Evolution of the DS temporal width (a) and intensity (b), in the vicinity of stability threshold (i.e., minimal κ, as pointed by circles in Fig. 2, 3), for the parameters of Fig. 2, 3, b.

Figs. 4–7 demonstrate the numerically computed evolution of the DS temporal width υ and intensity α^2, as a function of propagation distance Z. The calculations show the presence of three types of instability: i) a breathing behaviour in the vicinity of the threshold $\kappa \doteq \kappa_{min}$, ii) LB collapse, and iii) LB decay. However, the fundamental mode approximation cannot intrinsically describe the possible excitation of higher-order spatial modes. Therefore, direct numerical solutions of Eq. (1) are required.

III. NUMERICAL SOLITON SOLUTIONS

In our numerical simulations of Eq. (1), we used the COMSOL 5.4 software, the generalized alpha finite-element method (FEM) realized by the PARDISO solver on a rectangular mesh, with carefully optimized mesh and step sizes. The overall computational time for Z =5000

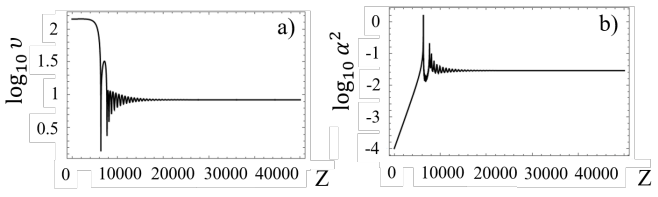

FIG. 7. Evolution of the DS temporal width (a) and intensity (b) in the vicinity of the stability threshold, for τ =0.1, Λ = −0.001, ν =0.01, and κ =0.000525.

TABLE I. Stability properties of DSs, and the corresponding minimum graded dissipation parameter κ_{min}.

Λ	τ	ν	κ_{min}
-0.01	0.01	0	0.00985
-0.01	0.01	0.001	0.0095
-0.01	0.01	0.01	0.009
-0.01	0.01	0.1	0.00675
-0.01	0.1	0	0.00975
-0.01	0.1	0.001	0
-0.01	0.1	0.01	0
-0.01	0.1	0.1	no solutions
-0.001	0.01	0	0.0008
-0.001	0.01	0.001	0
-0.001	0.01	0.01	0
-0.001	0.01	0.1	no solutions
-0.001	0.1	0	0.000525
-0.001	0.1	0.001	no stable solutions
-0.001	0.1	0.01	no stable solutions
-0.001	0.1	0.1	no solutions
-0.01	0.01	$\nu < 0$	no stable solutions
-0.01	0.1	$\nu < 0$	no stable solutions
-0.001	0.01	$\nu < 0$	no stable solutions
-0.001	0.1	$\nu < 0$	no stable solutions

depends on the window size, and takes about 4 – 6 hours on a Xeon 16-kernel server.

A. ST DS in the absence of "external phase-modulation" ($\nu = 0$)

Our analysis demonstrates that the spatially composed structure of a ST DS manifests itself in the form of spatiotemporal breathing of the LB, when κ tends to the stability threshold (see Fig. 8, here the threshold $\kappa \approx 0.0005$ in Table 1 is calculated from (A1–A5)). LB preserves its integrity, but compact doughnut- and pancake-like spatial structures occasionally appear, which introduce a long linear tail in the spectrum of the maximum intensity oscillations (see inset in Fig. 8, which shows the Fourier spectrum of the fine-grained maximum intensity dynamics). The growth of dissipation grading (i.e., the $\kappa-$parameter, see Fig. 9) suppresses multimode breathing, and leads to the formation of higher-order mode structures. A long high-frequency tail in the spectrum, as shown in Fig. 9, corresponds to the initial transient dynamics: the apparent spectral power decay is only the artefact of the limited simulation range (e.g., see inset in Fig. 10).

As it was pointed in [15], Eqs. (7) imply that spectral dissipation ("kinetic cooling") is a necessary condition for the existence of ST DSs. Table 1 demonstrates the squeezing the soliton stability range, when spectral dissipation ($\tau-$parameter in Eq. (1)) decreases. Numerical simulations confirm this claim. For instance, Fig. 9 shows a slower variation of the maximum intensity, when compared with the case of with Fig. 10.

An additional aspect of ST DS stabilization by spectral dissipation is connected with the weakening of the LB dependence on initial conditions (see Appendix B). Fig. 10 demonstrates that, as the value of τ is reduced, temporal splitting of the DS occurs, accompanied by an initial intensity decrease. The growth of $\tau-$ relaxes such a dependence of the LB on initial conditions: the LB-splitting disappears, and an improved convergence to the analytical solution is observed (see Fig. 9).

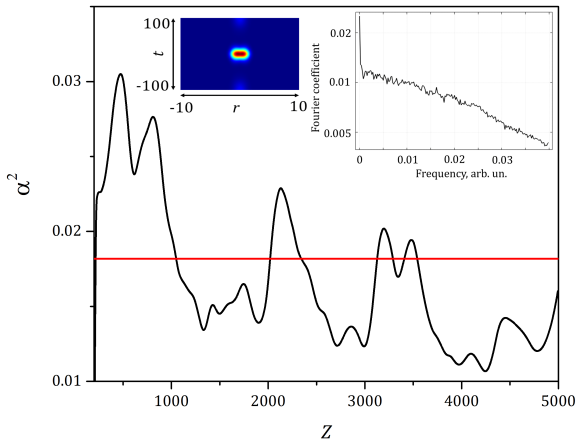

FIG. 8. Averaged evolution of the maximum intensity for τ =0.1, Λ = −0.001, ν =0, and κ =0.0007. Insets show the contour plot of the LB at Z =5000, and the spectrum of maximum intensity oscillations within $Z \in [0, 5000]$. The solid red line indicates the asymptotic intensity value, as it is obtained from the variational approximation.

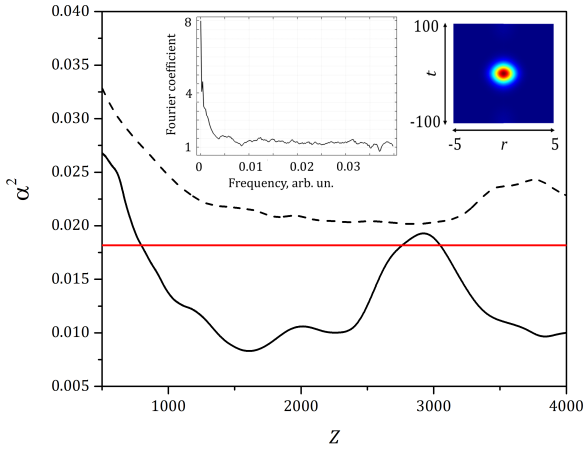

FIG. 9. Averaged evolution of the maximum intensity for τ =0.1, $\Lambda = -0.001$, ν =0, and κ =0.00085. Insets show the contour plot of LB at Z =5000, and the spectrum of maximum intensity oscillations within $Z \in [0, 5000]$. The solid red line indicates the asymptotic intensity value, as it is obtained from the variational approximation. The dashed curve shows the averaged intensity evolution corresponding to a threefold reduction of the initial intensity (*const* = 0.3 in Eq. (B1), see Appendix)

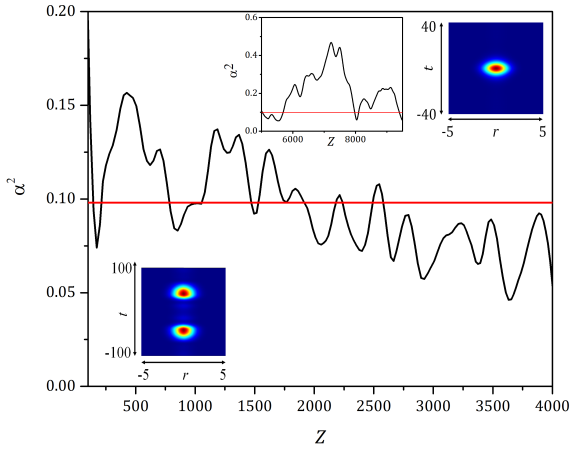

FIG. 10. The averaged evolution of the maximum intensity for τ =0.01, $\Lambda = -0.001$, ν =0, and κ =0.00085. The upper insets show the contour plot of LB at Z =5000 (right) and the prolonged maximum intensity evolution (left). The bottom inset shows the contour plot of the LBs power at Z =5000 for the threefold reduced initial intensity (*const* = 0.3 in Eq. (B1), see Appendix).

B. ST DS with "external phase-modulation"

The "external phase-modulation", defined the parameter ν in Eq. (1) introduces a temporal (i.e., $t-$dependent) localization of the refractive index, which corresponds to a 3D or pancake-like confining potential (see Fig. 1, *b*). In this sense, $\nu < 0$ breaks the ST confinement, so that there is no stable ST DS (see Table I). Numerical simulations confirm this statement.

Temporal confinement (i.e., $\nu > 0$) reduces the ST DS temporal duration, in agreement with analytical predictions (see Fig. 2 (b), and insets in Figs. 10, 11). This effect is physically understandable as follows. Namely, the additional phase shift νt^2 introduces a linear chirp on the propagating pulse. This shifts spectral components on the wings of the DS pulse, which then become closer to the edges of the parabolic gain-band. This increase losses on the temporal wings of the DS, and causes its temporal narrowing. At the same time, phase modulation may even suppresses the DS for large values of τ, i.e., in the case of a narrow gain bandwidth (see Table I). Our numerical simulations confirm this conclusion.

Our full numerical simulations reveal the presence of two effects, which are beyond predictions of the analytical solution of the variational approach. Firstly, the variational analysis predicts a decrease of the LB energy as the dissipation gradient parameter κ grows larger (see Fig. 3): this results from the degradation of the DS peak intensity. Such result agrees with numerical results (see Fig. 11). However, full simulations (black

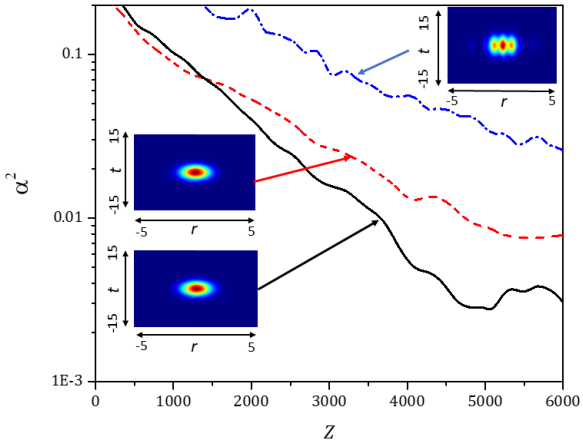

FIG. 11. Averaged evolution of the maximum intensity for τ =0.01, $\Lambda = -0.001$, ν =0.01, and κ =0.00085 (black solid), 0.0007 (red dashed), 0.0004 (blue dashed-dot). The insets show the contour plots of the LBs power at Z =6000 for the parameters corresponding to the curves indicated by arrows (*const* = 1 in Eq. (B1), see Appendix).

solid and red dashed curves, and corresponding insets in Fig. 11) demonstrate the existence of a "decreasing intensity" ST DS in what is a "forbidden region" of the $\kappa-$parameter (as far as the variational analysis prediction is concerned). The ST DS (see solid black and red dashed curves in Fig. 11) appear to reach a stable inten-

sity level after an initial slow decay.

Secondly, numerical simulations demonstrate that the temporally compressed ST DS, which is formed at a low values of κ, has a complex spatial structure (see the upper inset in Fig. 11). Such a spatial structure cannot be simply described in terms of the fundamental mode ansatz (2). Nevertheless, the spatial structure of the LB remains well-localized, without exhibiting any temporal splitting, and its averaged properties agree qualitatively with the analytical predictions.

IV. CONCLUSIONS AND OUTLOOK

In our work, we considered two-dimensional $(r-t)$ spatiotemporal dissipative solitons with confinement in both spatial and temporal dimensions. Such a confinement potential corresponds to a pancake-like potential in Bose-Einstein condensates, or to external synchronous phase modulation in graded-index multimode fiber lasers. In the last case, the $r-$coordinate is a transverse radial coordinate in an axially symmetrical fibers, and the $t-$coordinate corresponds to a local time in a coordinate frame moving with the pulse. This potential is enhanced by a dissipative cigar-type shape, which corresponds to weakly-dissipative Bose-Einstein condensates, or to multimode fiber lasers.

We based our analysis on the (2+1)-dimensional dissipative Gross-Pitaevskii equation, that was solved by both analytical and numerical approaches. In the first case, we used the variational approximation with the Gaussian-mode soliton ansatz. In the second case, a direct numerical simulation based on the finite-element method was performed.

In terms of photonics, we found that some minimal curvature of the graded dissipative potential (the $\kappa-$ parameter in Eq. (1)) is required to stabilize a ST soliton ("light bullet") against multimode beatings. Moreover, the growth of spectral dissipation (the $\tau-$ parameter in Eq. (1)), induced by a spectral filter or finite gain bandwidth, contributes to such stabilization, and suppresses multipulsing effects.

Synchronous external phase-modulation in a fiber laser leads to confinement in the temporal dimension, and relaxes the dependence of the light bullet stability on the graded dissipative potential. This means that a light bullet could be stabilized with weaker graded dissipation, and it exhibits significant temporal compression. However, the spatial structure of a light bullet for a low grading of the dissipative potential may acquire a complex multimode pattern.

Our findings suggest the following roadmap for the control of spatiotemporal dissipative solitons: i) A 3D confinement potential could be used, which involves a temporal localization of the gain. This can be achieved by including external phase modulation in a fiber laser cavity; ii) The multiscale nature of the light bullet dynamics, involving both "fast" $(t-)$ and "slow" $(Z-)$ coordinates should be exploited. In general, all parameters in Eq. (1) could become $(Z-t)$- dependent. Indeed, it was shown that the strategy of parameter management could stabilize spatiotemporal solitons [57]; iii) It should be noted that the numerical aperture, connected with a wave-front curvature, can be significant in multimode fiber lasers. In this case, the paraxial approximation underlying the derivation of Eq. (1) may be invalid, and the generalized Helmholtz equation should be used for the description of the transverse dynamics of MMF lasers.

ACKNOWLEDGMENTS

This work has received funding from the European Union Horizon 2020 research and innovation program under the Marie Skłodowska-Curie grant No. 713694 (MULTIPLY) and the ERC Advanced Grant No. 740355 (STEMS).

Appendix A: Evolution of DS parameters

The variational approximation based on Eqs. (2–6) results in the following ordinary differential equations for the evolving parameters of the DS:

$$\frac{d\theta}{dZ} = \frac{1}{6}\left(3+\frac{\alpha(Z)^2}{\rho(Z)^2}+12\theta(Z)^2-\frac{3}{\rho(Z)^4}\right), \tag{A1}$$

$$\frac{d\psi}{dZ} = \frac{3\alpha(Z)^2-4\left(3+\pi^2\right)\tau\psi(Z)}{3\pi^2\upsilon(Z)^2}-\frac{2}{\pi^2\upsilon(Z)^4}+ +\nu+2\psi(Z)^2, \tag{A2}$$

$$\frac{d\alpha}{dZ} = \frac{1}{15}\alpha(Z)\left(3\pi^2\upsilon(Z)^2\psi(Z)^2-\frac{5\left(12+\pi^2\right)\tau}{\pi^2\upsilon(Z)^2}\right)+ +\frac{1}{15}\alpha(Z)\left(15(\psi(Z)+2\theta(Z)-\Lambda\right), \tag{A3}$$

$$\frac{d\upsilon}{dZ} = \frac{8\tau}{\pi^2\upsilon(Z)}-2\upsilon(Z)\psi(Z)-\frac{16}{15}\pi^2\tau\upsilon(Z)^3\psi(Z)^2, \tag{A4}$$

$$\frac{d\rho}{dZ} = -\rho(Z)\left(2\theta(Z)+\kappa\rho(Z)^2\right). \tag{A5}$$

The physical steady-state solutions of this system are expressed by Eqs. (7–8) [56].

Appendix B: Initial conditions for FEM

As the initial conditions for the FEM simulations, we used the scalable expression for a DS amplitude, the soliton relation between temporal width and amplitude, and the LB relation between beam width and amplitude [53, 56]:

$$\alpha_0 = const\sqrt{\frac{3\left(\kappa^2-\Lambda^2-\Lambda^4\right)}{\kappa\Lambda}}, \tag{B1}$$

$$\upsilon_0 = \sqrt{2}\Big/\alpha_0, \tag{B2}$$

$$\rho_0 = \frac{1}{6}\left(\sqrt{\alpha_0^4+36}-\alpha_0^2\right). \tag{B3}$$

The initial spatial and temporal chirps (i.e., θ and ψ) were set as equal to zero.

[1] M. C. Cross and P. C. Hohenberg, Pattern formation outside of equilibrium, Rev. Mod. Phys. **65**, 851 (1993).
[2] L. Lugiato, Spatio-temporal structures. part i, Physics Reports **219**, 293 (1992).
[3] C. Weiss, Spatio-temporal structures. part ii. vortices and defects in lasers, Physics Reports **219**, 311 (1992).
[4] Y. Silberberg, Collapse of optical pulses, Opt. Lett. **15**, 1282 (1990).
[5] B. A. Malomed, D. Mihalache, F. Wise, and L. Torner, Spatiotemporal optical solitons, Journal of Optics B: Quantum and Semiclassical Optics **7**, R53 (2005).
[6] F. W. Wise, Generation of light bullets, Physics **3**, 107 (2010).
[7] V. S. Bagnato, D. J. Frantzeskakis, P. G. Kevrekidis, B. A. Malomed, and D. Mihalache, Bose-Einstein condensation. twenty years after, Romanian Reports in Physics **67**, (2015).
[8] Y. V. Kartashov, G. E. Astrakharchik, B. A. Malomed, and L. Torner, Frontiers in multidimensional self-trapping of nonlinear fields and matter, Nature Reviews Physics **1**, 185 (2019).
[9] P. A. Robinson, Nonlinear wave collapse and strong turbulence, Rev. Mod. Phys. **69**, 507 (1997).
[10] M. C. Marchetti, J.-F. Joanny, S. Ramaswamy, T. B. Liverpool, J. Prost, M. Rao, and R. A. Simha, Hydrodynamics of soft active matter, Reviews of Modern Physics **85**, 1143 (2013).
[11] A. Vespignani, Modelling dynamical processes in complex socio-technical systems, Nature physics **8**, 32 (2012).
[12] F. Abdullaev and V. V. Konotop, *Nonlinear waves: classical and quantum aspects*, Vol. 153 (Springer Science & Business Media, 2006).
[13] N. Akhmediev and A. Ankiewicz, *Dissipative solitons: from optics to biology and medicine*, Vol. 751 (Springer Science & Business Media, 2008).
[14] L. G. Wright, D. N. Christodoulides, and F. W. Wise, Spatiotemporal mode-locking in multimode fiber lasers, Science **358**, 94 (2017).
[15] V. L. Kalashnikov and S. Wabnitz, Distributed kerr-lens mode locking based on spatiotemporal dissipative solitons in multimode fiber lasers, Phys. Rev. A **102**, 023508 (2020).
[16] V. Kalashnikov and S. Wabnitz, A "metaphorical" nonlinear multimode fiber laser approach to weakly dissipative Bose-Einstein condensates, EPL (Europhysics Letters) **133**, 34002 (2021).
[17] D. J. Richardson, J. M. Fini, and L. E. Nelson, Space-division multiplexing in optical fibres, Nature photonics **7**, 354 (2013).
[18] P. Del'Haye, A. Schliesser, O. Arcizet, T. Wilken, R. Holzwarth, and T. J. Kippenberg, Optical frequency comb generation from a monolithic microresonator, Nature **450**, 1214 (2007).
[19] T. J. Kippenberg and K. J. Vahala, Cavity optomechanics: back-action at the mesoscale, Science **321**, 1172 (2008).
[20] P. Kelley, Self-focusing of optical beams, Physical Review Letters **15**, 1005 (1965).
[21] J. M. Dudley, F. Dias, M. Erkintalo, and G. Genty, Instabilities, breathers and rogue waves in optics, Nature Photonics **8**, 755 (2014).
[22] E. Turitsyna, S. Smirnov, S. Sugavanam, N. Tarasov, X. Shu, S. Babin, E. Podivilov, D. Churkin, G. Falkovich, and S. Turitsyn, The laminar–turbulent transition in a fibre laser, Nature Photonics **7**, 783 (2013).
[23] K. Krupa, A. Tonello, A. Barthélémy, T. Mansuryan, V. Couderc, G. Millot, P. Grelu, D. Modotto, S. A. Babin, and S. Wabnitz, Multimode nonlinear fiber optics, a spatiotemporal avenue, APL Photonics **4**, 110901 (2019).
[24] F. O. Wu, A. U. Hassan, and D. N. Christodoulides, Thermodynamic theory of highly multimoded nonlinear optical systems, Nature Photonics **13**, 776 (2019).
[25] B. A. Malomed, Multidimensional solitons: Well-established results and novel findings, The European Physical Journal Special Topics **225**, 2507 (2016).
[26] O. V. Shtyrina, M. P. Fedoruk, Y. S. Kivshar, and S. K. Turitsyn, Coexistence of collapse and stable spatiotemporal solitons in multimode fibers, Physical Review A **97**, 013841 (2018).
[27] K. Krupa, A. Tonello, B. M. Shalaby, M. Fabert, A. Barthélémy, G. Millot, S. Wabnitz, and V. Couderc, Spatial beam self-cleaning in multimode fibres, Nature Photonics **11**, 237 (2017).
[28] W. H. Renninger and F. W. Wise, Optical solitons in graded-index multimode fibres, Nature communications **4**, 1 (2013).
[29] P. Grelu, J. M. Soto-Crespo, and N. Akhmediev, Light bullets and dynamic pattern formation in nonlinear dissipative systems, Optics express **13**, 9352 (2005).
[30] V. Skarka and N. Aleksić, Stability criterion for dissipative soliton solutions of the one-, two-, and three-dimensional complex cubic-quintic Ginzburg-Landau equations, Physical review letters **96**, 013903 (2006).
[31] H. Leblond, B. A. Malomed, and D. Mihalache, Stable vortex solitons in the Ginzburg-Landau model of a two-dimensional lasing medium with a transverse grating, Physical Review A **80**, 033835 (2009).
[32] D. Mihalache, D. Mazilu, V. Skarka, B. Malomed, H. Leblond, N. Aleksić, and F. Lederer, Stable topolog-

ical modes in two-dimensional Ginzburg-Landau models with trapping potentials, Physical Review A **82**, 023813 (2010).
[33] B. A. Malomed, Spatial solitons supported by localized gain, JOSA B **31**, 2460 (2014).
[34] T. Bhutta, J. I. Mackenzie, D. P. Shepherd, and R. J. Beach, Spatial dopant profiles for transverse-mode selection in multimode waveguides, JOSA B **19**, 1539 (2002).
[35] C.-K. Lam, B. Malomed, K. Chow, and P. K. A. Wai, Spatial solitons supported by localized gain in nonlinear optical waveguides, The European Physical Journal Special Topics **173**, 233 (2009).
[36] V. E. Lobanov, O. V. Borovkova, Y. V. Kartashov, V. A. Vysloukh, and L. Torner, Topological light bullets supported by spatiotemporal gain, Physical Review A **85**, 023804 (2012).
[37] U. Teğin, E. Kakkava, B. Rahmani, D. Psaltis, and C. Moser, Spatiotemporal self-similar fiber laser, Optica **6**, 1412 (2019).
[38] H. G. Winful and D. T. Walton, Passive mode locking through nonlinear coupling in a dual-core fiber laser, Optics letters **17**, 1688 (1992).
[39] A. Aceves, C. De Angelis, A. M. Rubenchik, and S. K. Turitsyn, Multidimensional solitons in fiber arrays, Optics letters **19**, 329 (1994).
[40] J. Proctor and J. N. Kutz, Nonlinear mode-coupling for passive mode-locking: application of waveguide arrays, dual-core fibers, and/or fiber arrays, Optics express **13**, 8933 (2005).
[41] T. F. Büttner, D. D. Hudson, E. C. Mägi, A. C. Bedoya, T. Taunay, and B. J. Eggleton, Multicore, tapered optical fiber for nonlinear pulse reshaping and saturable absorption, Optics letters **37**, 2469 (2012).
[42] That claim appears to be trivial for BEC bosons, but it is not obvious for massless photons [58, 59].
[43] W. H. Renninger and F. W. Wise, Spatiotemporal soliton laser, Optica **1**, 101 (2014).
[44] J. Zhang, J. Brons, M. Seidel, D. Bauer, D. Sutter, V. Pervak, V. Kalashnikov, Z. Wei, A. Apolonski, F. Krausz, and O. Pronin, Generation of 49-fs pulses directly from distributed Kerr-lens mode-locked Yb:YAG thin-disk oscillator, in *Advanced Solid State Lasers* (Optical Society of America, 2015) p. ATh4A.7.
[45] C. R. Doerr, H. A. Haus, E. P. Ippen, M. Shirasaki, and K. Tamura, Additive-pulse limiting, Opt. Lett. **19**, 31 (1994).
[46] N. Smith, K. Blow, W. Firth, and K. Smith, Soliton dynamics in the presence of phase modulators, Optics Communications **102**, 324 (1993).
[47] V. Kalashnikov, I. Poloiko, and V. Mikhailov, Phase modulation of radiation of solid-state lasers in the presence of Kerr optical nonlinearity, Optics and Spectroscopy **84**, 104 (1998).
[48] S. Wabnitz, Suppression of soliton interactions by phase modulation, Electronics Letters **29**, 1711 (1993).
[49] W. Chang, N. Akhmediev, S. Wabnitz, and M. Taki, Influence of external phase and gain-loss modulation on bound solitons in laser systems, J. Opt. Soc. Am. B **26**, 2204 (2009).
[50] Despite the statement in [25]: "it is virtually impossible to impose modulation of the refractive index providing the trapping in the temporal direction".
[51] Y. V. Bludov and V. Konotop, Nonlinear patterns in Bose-Einstein condensates in dissipative optical lattices, Physical Review A **81**, 013625 (2010).
[52] P. Fedichev, Y. Kagan, G. Shlyapnikov, and J. Walraven, Influence of nearly resonant light on the scattering length in low-temperature atomic gases, Physical review letters **77**, 2913 (1996).
[53] S. Raghavan and G. P. Agrawal, Spatiotemporal solitons in inhomogeneous nonlinear media, Optics Communications **180**, 377 (2000).
[54] S.-S. Yu, C.-H. Chien, Y. Lai, and J. Wang, Spatiotemporal solitary pulses in graded-index materials with Kerr nonlinearity, Optics communications **119**, 167 (1995).
[55] A. Ankiewicz, N. Akhmediev, and N. Devine, Dissipative solitons with a lagrangian approach, Optical Fiber Technology **13**, 91 (2007).
[56] V. L. Kalashnikov, *Variational approach to a fiber-laser spatial-temporal dissipative soliton: 3D-confinement (Mathematica 12.1 notebook)* (2021), `http://info.tuwien.ac.at/kalashnikov/DKLM3D.nb`.
[57] T. Mayteevarunyoo, B. A. Malomed, and D. V. Skryabin, Spatiotemporal solitons in dispersion-managed multimode fibers, Journal of Optics **23**, 015501 (2020).
[58] A. Fratalocchi, Light condensation, Nature Photonics **4**, 502 (2010).
[59] D. N. Sob'yanin, Bose-Einstein condensation of light: General theory, Physical Review E **88**, 022132 (2013).